The Astronomical Journal, 118:705–718, 1999 August

AN INFRARED SEARCH FOR EXTINGUISHED SUPERNOVAE IN STARBURST GALAXIES

Bruce Grossan,[1] Earl Spillar,[2] Robert Tripp,[3] Norbert Pirzkal,[4] Brian M. Sutin,[5] Paul Johnson,[2] and David Barnaby[6]

Received 1998 December 14; accepted 1999 April 7

ABSTRACT

IR and radio-band observations of heavily extinguished regions in starburst galaxies suggest a high supernova (SN) rate associated with such regions. Optically measured SN rates may therefore underestimate the total SN rate by factors of up to 10, as a result of the very high extinction ($A_B \sim$ 10–20 mag) to core-collapse SNe in starburst regions. The IR/radio SN rates come from a variety of indirect means, however, which suffer from model dependence and other problems. We describe a direct measurement of the SN rate from a regular patrol of starburst galaxies done with K'-band imaging to minimize the effects of extinction. A collection of K'-band measurements of core-collapse SNe near maximum light is presented. Such measurements (excluding 1987A) are not well reported in the literature. Results of a preliminary K'-band search, using the MIRC camera at the Wyoming Infrared Observatory and an improved search strategy using the new ORCA optics, are described. A monthly patrol of a sample of *IRAS* bright (mostly starburst) galaxies within 25 Mpc should yield 1–6 SNe yr^{-1}, corresponding to the range of estimated SN rates. Our initial MIRC search with low resolution (2″.2 pixels) failed to find extinguished SNe in the *IRAS* galaxies, limiting the SN rate outside the nucleus (at greater than 15″ radius) to less than 3.8 far-IR SN rate units (SNe per century per 10^{10} $L_\odot$ measured at 60 and 100 μm, or FIRSRU) at 90% confidence. The MIRC camera had insufficient resolution to search nuclear starburst regions, where starburst and SN activity is concentrated; therefore, we were unable to rigorously test the hypothesis of high SN rates in heavily obscured star-forming regions. We conclude that high-resolution nuclear SN searches in starburst galaxies with small fields are more productive than low-resolution, large-field searches, even for our sample of large (often several arcminutes) galaxies. With our ORCA high-resolution optics, we could limit the total SN rate to less than 1.3 FIRSRU at 90% confidence in 3 years of observations, lower than most estimates.

Key words: dust, extinction — galaxies: nuclei — galaxies: starburst — infrared radiation — instrumentation: miscellaneous — supernovae: general

1. INTRODUCTION

1.1. *Limitations of Optical Supernova Searches*

A number of efforts to measure the frequency of supernovae (SNe) have been made that include systematic recording of observation times and sensitivities and a relatively well defined sample of galaxies (e.g., Muller et al. 1992; Evans, van den Bergh, & McClure 1989; Capellaro & Turatto 1988). These works have all used optical observations, usually in *B*. Such observations cannot detect SNe behind significant amounts of dust, such as those occurring in dusty star formation regions, because the dust causes up to tens of magnitudes of extinction in the optical bands. It is difficult to correct optical rate measurements for this effect, since some estimates (discussed below) suggest that SNe in these regions could dominate the total rate. For this reason, SN rate measurements from optical observations can only be lower limits to the true rate. The SN rate from optical measurements (see the first section of Table 1) is 0.74–1.6 blue supernova rate units (BSRU), where 1 BSRU = 1 SN per century per 10^{10} $L_{B,\odot}$ and $L_{B,\odot}$ is the unit of solar luminosity measured in the *B* band (Capellaro & Turatto 1988, for example, refer to this unit as the SNu, but this term can be confused with the solar neutrino unit or SNU from, e.g., Bahcall 1989). A rough estimate of the number of SNe per century in a galaxy similar to our own is about 1 BSRU. The rate of core-collapse SNe (non–Type Ia SNe) dominates the total rate measurement in late-type galaxies (see, e.g., Muller et al. 1992).

1.2. *The Extinguished-SN Hypothesis*

Basic stellar evolution predicts that massive stars ($\gtrsim 8$ $M_\odot$; Woosley & Weaver 1986) burn their nuclear fuel rapidly and end their lives in a core-collapse SN in a short time (about $10^{7.1}$–$10^{7.5}$ yr for stars initially of 8–15 $M_\odot$; Schaller et al. 1992). The progenitors of these core-collapse SNe are therefore found primarily in active star-forming regions, as they will explode before the burst is over (the $1/e$ time of the star formation in the burst is $\sim 10^{7.3}$–10^{8} yr; Rieke et al. 1980). The extinctions to stars in the largest star-forming regions, those in "starburst" galaxies, are measured to be approximately 14–25 mag (as measured for NGC 253 and M 82, respectively; Rieke et al. 1980) in visual bands. Enormous far-IR luminosities are observed for starburst galaxies as a result of dust absorption and reemission of light from these luminous stars. Accounting for the

[1] Space Sciences Laboratory, University of California, Berkeley; and Institute for Nuclear and Particle Astrophysics, Lawrence Berkeley National Laboratory, 1 Cyclotron Road, Mail Stop 50-232, Berkeley, CA 94720; bruce@singu.lbl.gov.

[2] Department of Physics and Astronomy, University of Wyoming, P.O. Box 3905, University Station, Laramie, WY 82071; spillar@uwyo.edu, pjohnson@uwyo.edu.

[3] Physics Division, Lawrence Berkeley National Laboratory, 1 Cyclotron Road, Mail Stop 50-348, Berkeley, CA 94720; rtripp@lbl.gov.

[4] European Southern Observatory, Karl-Schwarzschild-Strasse 2, D-85748 Garching bei München, Germany; npirzkal@eso.org.

[5] University of California Observatories/Lick Observatory, Santa Cruz, CA 95064; sutin@ucolick.edu.

[6] Yerkes Observatory, 373 West Geneva Street, Williams Bay, WI 53191; barnaby@hale.yerkes.uchicago.edu.

TABLE 1

SN Rate Measurements

Rate		Basis	Reference	Comment
FIRSRU	BSRU			
		Optical Measurements		
	0.74	Optical	Capellaro & Turatto 1988 (Asiago search)	
	1.43	Optical	Evans et al. 1989	
	1.56	Optical	Muller et al. 1992	Type Ibc dominate, most found in spirals
	≈2 late-type (Sb–Im), ≈0.5 early-type (E–Sb)	Optical	van den Bergh & Tammann 1991	
		Unextinguished (Nonoptical) Measurements in Starbursts		
3	5	Radio	Kronberg & Wilkinson 1975	0.1 yr^{-1} in M 82
10	15	Modeled IMF to match radio, IR, optical, X-ray observations	Rieke et al. 1980	0.3 yr^{-1} in M 82, same rate in NGC 253; low-mass stars must be suppressed
6–10	10–16	Radio variability	Kronberg & Sramek 1985	0.2–0.3 yr^{-1} in M 82
>3	>9	Radio source counts and remnant ages in NGC 253	Antonucci & Ulvestad 1988	>0.1 SNe yr^{-1} in NGC 253
5	~8[a]	"Gas consumption rate"	Van Buren & Norman 1989	0.5 yr^{-1} 10–11 $L_{\odot}$ *IRAS* galaxy
< 3.4	<5	Age of radio source population and source counts[b]	Van Buren & Greenhouse 1994	<0.10 yr^{-1} in M 82, <0.08 yr^{-1} in NGC 253
<3.4	<5	Radio variability	Ulvestad & Antonucci 1994	<0.10 yr^{-1} in M 82, <0.25 yr^{-1} in NGC 253
1.7	2.6	SNR number vs. diameter relation	Muxlow et al. 1994	0.05 yr^{-1} in M 82
1.6[c]	6[c]	[Fe II] (1.26 μm) luminosity	Engelbracht et al. 1998	0.03 yr^{-1} in NGC 253[c]
>0.4	>1.5	SNR radio size = age	Allen & Kronberg 1998	>0.016 yr^{-1} in M 82

[a] The BSRU number was determined assuming the ratio of L_B/L_{FIR} for M 82.

[b] The authors used log N–log S arguments to throw away some Antonucci & Ulvestad sources.

[c] The authors report 0.03 yr^{-1} in NGC 253, but from a luminosity-dependent measure that used $d = 2.5$ Mpc to NGC 253. We therefore divided their luminosity-dependent number of SN by the luminosity using their distance to obtain the SN rate in SRU (whereas we used our value of $d = 3.6$ Mpc, and the associated luminosity in the other rows with NGC 253 measurements). Note that the authors themselves point out that their value is discrepant with other measurements unless they adopt $d = 3.5$ Mpc.

observed spectrum shows that starburst galaxies harbor the largest populations of massive SN progenitor stars, particularly in their circumnuclear regions (Rieke et al. 1980). The *majority* of supernova progenitors are therefore undetectable with optical measurements in this simple hypothesis. Even a very recent optically based measurement of the SN rate, specifically in starburst galaxies, found a rate similar to that measured in "normal" galaxies (0.7 h^2 BSRU for Type Ibc and $\sim$0.6 h^2 BSRU for Type II; Richmond, Filippenko, & Galisky 1998). Optical measurements may therefore be significantly underestimating the true rate of SNe (e.g., Van Buren & Norman 1989).

The SN rate is important for understanding nucleosynthesis, the abundance of metals, and the structure of the interstellar medium. It is also important in the study of SNe themselves. Observations of SNe by gravitational-wave and neutrino detectors would give us important new tools with which to study this phenomenon. To design such devices effectively for observation of SNe, however, one first needs to know the frequency of nearby SNe, including those that may be extinguished. In this paper, we describe a search for extinguished SNe, using observations in the near-IR to overcome detection bias due to extinction. We present our observing strategy, expected event rate, preliminary results, and plans for an improved search.

2. EVIDENCE FOR EXTINGUISHED SUPERNOVAE

The BSRU rate measure allows us to predict the SN rate in a given galaxy with negligible internal extinction, given the BSRU rate for its galaxy type and its L_B. However, we propose a different rate per luminosity measure for dusty starburst galaxies. Massive stars in star-forming regions warm their enshrouding dust, so most of their radiation escapes in the far-IR and is detected in the *IRAS* 60 and 100 μm bands. The *IRAS* far-IR luminosity ($L_{\rm FIR}$; Soifer et al. 1987) of a starburst galaxy is therefore a good indicator of its population of extinguished massive SN progenitors (unless other unusual sources of far-IR radiation dominate, such as a Seyfert nucleus). How the $L_{\rm FIR}$ relates to the actual population of massive stars, e.g., stars with $M > 8\ M_\odot$, will actually depend on the distribution of dust, its composition, the size of the star-forming region, the initial mass function, and so forth. In this paper, we make the rough, preliminary assumption that in luminous starburst galaxies, $L_{\rm FIR}$ is a better indicator of the *total* massive stellar population than L_B, analogous to L_B in normal, relatively unextinguished galaxies. An SN rate prediction using $L_{\rm FIR}$ should therefore be better for luminous starbursts than one using L_B. (Type Ia SNe come from evolved stars in binary systems and are not related to the massive extinguished stars emphasized here. However, these events are rare compared with core-collapse SNe and would not affect the total rate much; see, e.g., Muller et al. 1992.) Kronberg, Biermann, & Schwab (1985) have shown that radio flux from compact sources in starburst nuclei (probably supernova remnants) correlates with 100 μm flux, supporting these assumptions. Accordingly, we define 1 FIRSRU = 1 SN per century per 10^{10} $L_{\rm FIR,\odot}$, where $L_{\rm FIR,\odot}$ is the unit of solar luminosity measured in the far-IR bands. After direct observations of the SN rate in starbursts, the predictive power of these two methods may be compared.

One can observe dusty regions in starburst galaxies in the radio and IR because the extinction is small in these bands. The propagation of radio waves is essentially unaffected by the presence of dust, and for Milky Way dust, the 2.2 μm K-band extinction is less than 1/10 that in the B band, measured in magnitudes ($A_K/A_B < 1/10$; Cardelli, Clayton, & Mathis 1989). The SN rate estimates based on such observations are summarized in the second part of Table 1. As expected, the BSRU values for starbursts are much higher than the BSRU rates for the starburst-poor samples in the first section. The values vary widely, from 1.6 to 10 FIRSRU, even though most of the measurements in the table were performed for the same galaxies, NGC 253 and M 82. The different measurement techniques do not agree.

Radio observations have yielded large numbers of bright compact sources consistent with young supernova remnants (SNRs) in the two nearby starburst galaxies M 82 and NGC 253 (Kronberg & Wilkinson 1975; Antonucci & Ulvestad 1988) and, more recently, in M 83 (Cowan, Roberts, & Branch 1994). However, radio measurements of fading and expansion of these SNRs would provide a more direct proof of their identity. Kronberg & Sramek (1985) showed that some of the sources are fading, providing an apparent confirmation. Ulvestad & Antonucci (1994), however, dispute the findings and suggest that some of the sources may be flat-spectrum sources (i.e., not SN related). (Note that radio observations of fading or expansion typically require a baseline of a decade or more, and the required measurements are difficult because of the crowding of sources in galaxy nuclei.) Muxlow et al. (1994) confirm that most sources are SNRs but derive a low SN rate based on an assumed expansion velocity. Van Buren & Greenhouse (1994) used a method of identifying SNRs and base an SN rate estimate on the age of the full population of SNe, which is claimed to be a more direct method of measurement.

Rieke et al. (1980) use IR imaging and spectroscopy to produce a model of the stellar populations in M 82 and NGC 253. In order for the model to be consistent with published radio, IR, UV, and X-ray data, an initial mass function heavily biased toward massive, young stars was required. A very high rate of extinguished SNe was therefore derived. The model dependence of this method may be the reason why it yields higher rates than the most recent radio-based results.

The observations clearly indicate that enhanced star formation is occurring in these starburst galaxies, and that there are large numbers of young, high-mass stars. The problem is that all of the SN rate estimates above have some model input and dependence. There can be little doubt that SNe do occur in extinguished starburst regions, however. An SN was discovered in the IR K (2.2 μm) band in the extremely IR-luminous galaxy NGC 3690 (SN 1992bu; Van Buren et al. 1994), i.e., right where one would expect such a detection. No optical detections of the SN were made in this frequently observed galaxy, consistent with heavy extinction to the SN. Unfortunately, no meaningful rate measurement can be derived from one event. The extinguished-SN hypothesis is therefore still without a robust confirmation or refutation, hence the motivation for our near-IR search.

3. IR LUMINOSITY OF CORE-COLLAPSE SNe

To determine the required sensitivity for our search, we need to know the average near-IR luminosity of core-collapse SNe. Unfortunately, there is a paucity of published near-IR measurements of core-collapse SNe near peak brightness. Most published near-IR measurements are of Type Ia events. Since the possibility of host galaxy reddening plagues optical measurements, we have chosen not to extrapolate these data to determine the luminosity. Instead, we have sought near-IR measurements from the literature and have added some of our own.

Detailed measurements of core-collapse SNe in the literature are dominated by studies of the nearby SN 1987A. This Type II is anomalous by many measures, including a greater than 100 day wide light-curve peak in the optical and near-IR bands, making the data on this SN of little value to us. This is *not* a case of " any object close enough to be well studied is anomalous "; the latter feature would be observed even if the SN were near the limits of detectability.

We were able to obtain near-IR measurements for five other core-collapse SNe—all except for one within a few days of maximum at K—from our own observations and from published measurements. These values are given in Table 2. Core-collapse SNe include Type Ib and Ic, which are relatively similar, and the various Type IIs, which have a large dispersion in their optical luminosities (Miller & Branch 1990, hereafter MB90). The optical Type Ib + Ic rate is 1.1 h^2 BSRU and the optical Type II rate is about 1.6 h^2 BSRU for spiral galaxies (Muller et al. 1992). It is therefore important to know the luminosity of both core-collapse Type I and Type IIs. Since the K'-band data of Panagia et al. (1986, private communication; widely circulated, unpublished paper on multifrequency observations of SN 1983N, 1986 August draft) sample a Type I core-collapse light curve fairly well near maximum light, we used these data as a light-curve template to estimate the maximum brightness of other Type I core-collapse light curves with limited sampling. From our knowledge of the time of B_{max} (maximum flux in the B band), we selected the measurement closest to the expected date of K_{max} in order to make the smallest correction. The one extrapolation in the table made the K_{max} of SN 1984L only 0.14 mag brighter than in our actual measurements. We did not apply corrections for Type II light curves.

We found the maximum K-band luminosities to be $M_{K,max} = -18.0$ for Type Ibc SNe (the average of 1994I measured 15 days after optical maximum, 1983N at its K_{max}, and SN 1984L corrected to K_{max}) and $M_{K,max} = -18.3$ for Type II SNe (the average of 1993J at V maximum + 12 days and 1980K at B_{max}). (We use $H_0 = 75$ km s^{-1} Mpc^{-1}.) Our data are probably slightly fainter than the true maximum, however, as the Type I core-collapse light curve of Panagia et al. might have missed K_{max} by a few days, and for Type IIs, we have no good way to correct the data to K_{max}. It should also be noted that optical measurements suggest that there is a large intrinsic dispersion in the luminosity of our SNe (see below). With so few measurements, our values are therefore only a rough estimate of the average luminosities. While we recognize the limitations of these estimates, note that they are much more appropriate than theoretical values or extrapolations from optical measurements for our purposes. We adopt a combined value of $M_{K,max} = -18.1$ for all core-collapse SNe in the absence of data that justifies subdividing them. Finally, note that the effect of extinction in K band must be insignificant here. The SNe used in the estimate above were all discovered optically and could not have been discovered if more than a few magnitudes of optical extinction were present. For a few magnitudes' extinction in the optical, the effect at K cannot be larger than a few tenths of a magnitude.

In contrast to the near-IR measurements, many SN light curves have been measured optically. Type Ibc SNe have a blue luminosity of $M_{B,max} = -17.1$ with $\sigma = 0.34$ dispersion, whereas Type II have $M_{B,max} = -16.9$ with the large dispersion of 1.35 mag (MB90, $H_0 = 75$ km s^{-1} Mpc^{-1}). (Note that Type Ibc is more luminous than Type II according to MB90, but conversely for our small number of IR measurements. This is consistent with the large dispersion in the luminosity of Type IIs.) Until more IR measurements are made, it will remain unclear whether this dispersion comes from variations in host environment extinction or whether it comes from intrinsic variations in SN luminosity.

4. OBSERVING PLAN AND PREDICTED DETECTION RATE

Now, using our luminosity value derived above, consider observations of SNe in high-extinction starburst regions. Assuming 2 mag of extinction at K (about 20 mag at B), the

TABLE 2

IR MEASUREMENTS OF CORE-COLLAPSE SNe

SN (galaxy)	Spectral Type	Distance[a] (Mpc) (ref.)	$M_{K,max}$	K_{max}	Measurement Date[b] (ref.)
1980K (NGC 6946)	II-L	5.5 (Buta)	−18.6	10.07	Nov 1 = $t(B_{max})$ (Dwek)
1984L (NGC 991)	Ib	18.8 (Tully)	−18.6	12.73 (corrected[c])	$t(K_{max})$[c] (Elias)
1983N (M 83 = NGC 5236)	Ib	4.7 (Tully)	−18.2	10.19	Jul 26 ≈ $t(K_{max})$ (Panagia)
1993J (M 81 = NGC 3031)	"IIb"[d]	3.6 (Freedman)	−18.0	9.82	Apr 18 = $t(V_{max}) + 12 \approx K_{max}$ (I5773)
1994I (M 51 = NGC 5194)	Ic	8.3 (Richmond)	−17.0	12.56	Apr 16 = $t(B_{max}) + 11 \approx K_{max}$ (this work)[e]

NOTE.—The average value of $M_{K,max}$ for Type Ib and Ic is -18.0 ± 0.48. The average value of $M_{K,max}$ for all Type IIs is -18.3 ± 0.34. The average value for all SNe together is $M_{K,max} = -18.1 \pm 0.30$.

[a] For all purposes in this paper, H_0 is taken to be 75 km s^{-1} Mpc^{-1}.

[b] $t(V_{max})$ or $t(B_{max})$ + some number gives the time of maximum light in the given filter plus the given number of days. Note that the time of maximum K-band brightness was ∼10 days past B_{max} in Panagia et al. (1986, private communication).

[c] Since the light curve for the Type Ib SN 1983N was well sampled near max by Panagia et al., we used their data as a template to correct the observations of SN 1984L. The daily changes relative to B max were used, with linear interpolation, to correct the observations ($K = 12.87$) to the maximum brightness. SN 1994I was measured close to the predicted IR max, and so no correction was made. No corrections were made to Type II light curves as no representative light-curve templates were available. See text for additional comments.

[d] A " IIb " refers to an SN Type II that exhibited Ib spectra at late time, with double maxima.

[e] These measurements were made at the University of Wyoming Observatory Telescope on UT 1994 April 16 with the Michigan IR Camera (MIRC). The measurements were made through a K' filter, and the corrections to the K band were assumed to be small.

REFERENCES.—Dwek = Dwek et al. (1983), Buta = Buta (1982), Tully = Tully (1988), Panagia = Panagia et al. (1986, private communication), Freedman = Freedman et al. (1994), I5773 = Romanishin in IAUC 5773, Richmond = Richmond et al. (1996).

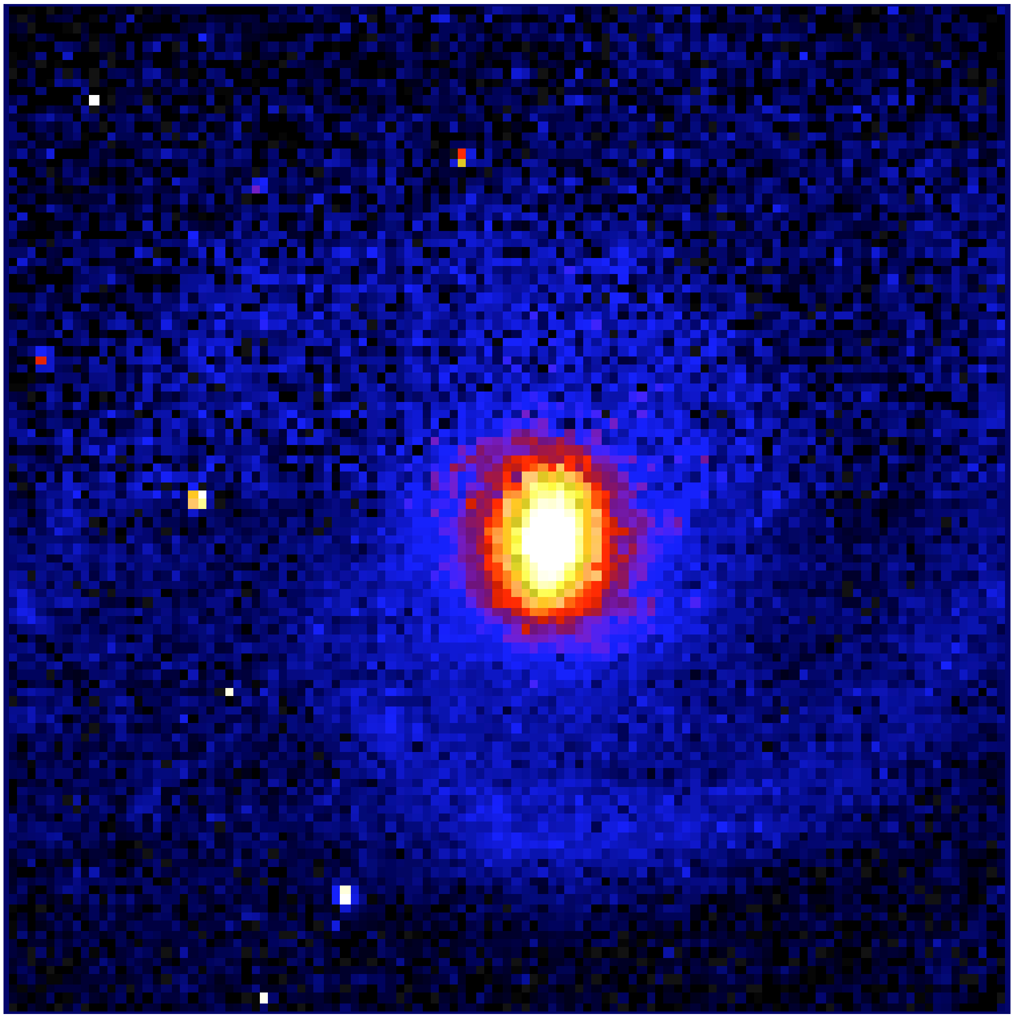

FIG. 1*a*

FIG. 1.—K'-band images of NGC 5194 (M 51) with the MIRC camera on the WIRO Telescope. (*a*) The reference image, taken 1994 March 2. (*b*) The galaxy after the explosion of SN 1994I, taken 1994 April 16. The SN is indicated by a light square around the object. (*c*) The results of registering, scaling, and subtracting the two images. The residual SN is obvious, but significant noise is present at the location of the galaxy center. The image scale is 2″.2 pixel^{-1}. The detector chip was not oriented parallel to standard compass directions. The SN is located 14″ east and 12″ south of the nucleus (Richmond et al. 1996). Roughly speaking, north is at upper right and east is at lower right. [*See the electronic edition of the Journal for a color version of Fig. 1c.*]

average core-collapse SN would have $K = 15.9$ at a distance of about 25 Mpc (distance modulus $= 32.0$). Detecting a point source of this brightness is a modest task for modern detectors and IR-optimized telescopes. A more critical factor is whether or not there are enough SNe within the volume one can search to make a meaningful measurement of the SN rate.

We consider a sample of 177 FIR-selected *IRAS* catalog galaxies within 25 Mpc, which are visible from our Northern Hemisphere observatory ($\delta > -20$), for a measurement of the local SN rate. We chose FIR selection so that the sample would be dominated by starbursts, a condition for our assumptions above. Some of the galaxies may not be dominated by radiation from starburst regions (a few have active galactic nuclei that also emit powerfully in the FIR); however, the starburst galaxies are the most luminous, and so the aggregate luminosity is certainly dominated by radiation from starbursts. We predict the expected number of observed SNe for a given starburst galaxy to be the FIR rate times L_{FIR} for the given galaxy multiplied by the cumulative visibility time. A single observation's visibility time is the lesser of the time until the next observation and the time for which an SN would be detectable at the distance of the given galaxy. Core-collapse SN K-band light curves have a fairly broad peak and typically stay within about 0.3 mag of peak for 1 month (e.g., Panagia et al. 1986, private communication; Elias et al. 1985; Dwek et al. 1983; Suntzeff & Bouchet 1991), allowing us to efficiently observe only once per month. When two consecutive observations are not achieved, we take the control time for the last observation to be one month. Using the range of 1.6–10 FIRSRU given in the table for our starbursts and considering when during the year one can observe a given galaxy, 1.6–9.6 SNe yr^{-1} should be observed within our 25 Mpc sample. (In those cases where L_{FIR} was not given in Soifer et al. 1987, we generated these values from the distances in Table A1 in the Appendix and the fluxes given in the *IRAS* Faint Source Catalog.)

5. OBSERVATIONS OF NEARBY STARBURST GALAXIES

Between 1992 and 1994, we performed observations on the 2.3 m Wyoming IR Observatory (WIRO) telescope in

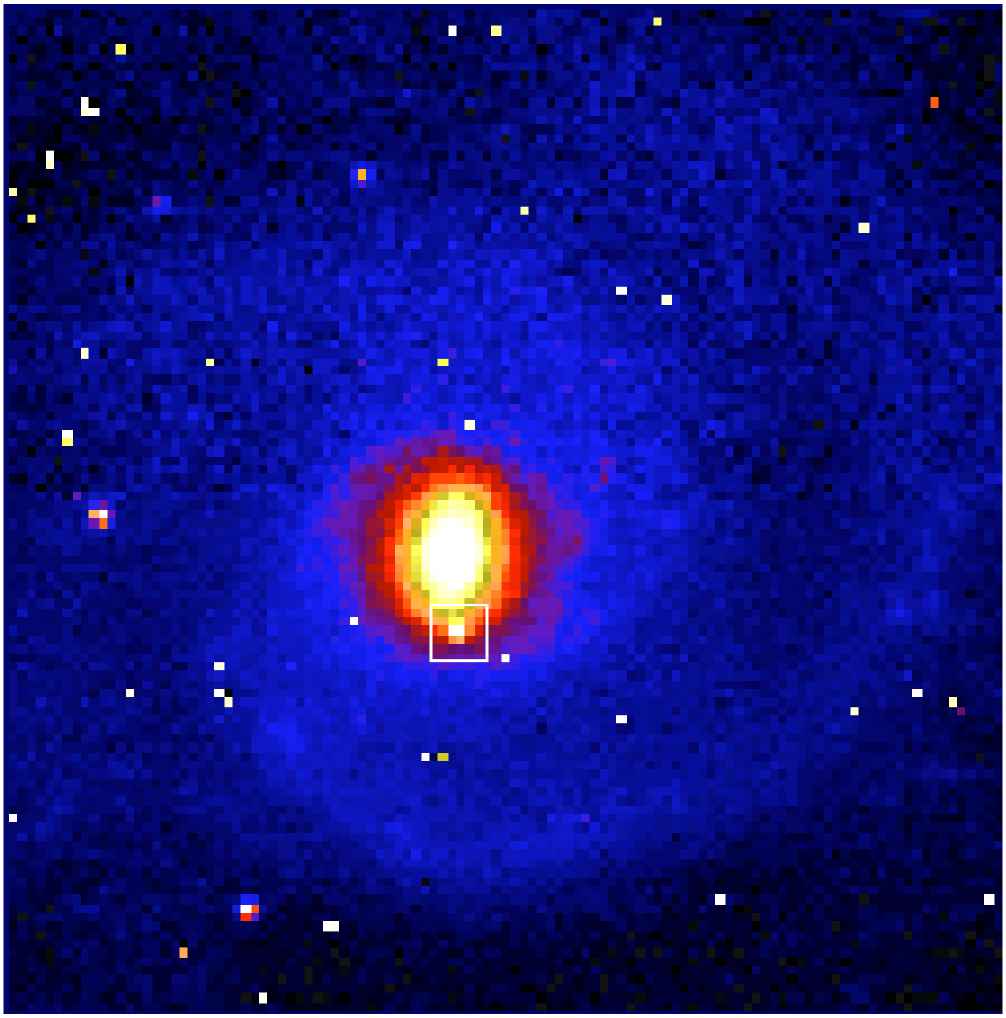

FIG. 1b

the K' band. (The K' band is centered at 2.1 μm, about 0.1 μm short of the K-band center, sampling nearly the same band but with less thermal instrument background.) The best instrument then available was the MIRC (Michigan IR camera), with a 128 × 128 HgCdTl detector. At prime focus the instrument had a 2.″2 pixel size. We were able to patrol more than 75 galaxies per night under good conditions, and we were granted five nights per month most months.

Although the background noise can vary with the outside temperature, we would typically measure a background noise per pixel of $\sigma_1 = 18.0 + 1.25 \log [t_{\rm exp}/(180 \text{ s})]$ mag. The noise scales simply with square root of exposure time, $t_{\rm exp}^{1/2}$, in at least the range 30–240 s, where the sky background dominates the read noise, and shutter and other effects are negligible. We use a 2 pixel aperture because with 0.″7 typical seeing and 2.″2 pixels, a point source has most of the flux in a single pixel. There is frequently minor spillover into a second pixel, but it is rare for significant flux to be in a third or more pixels. Multiplying the noise by the square root of 2 for the second pixel and converting to magnitudes yields $\sigma_2 = 17.6 + 1.25 \log [t_{\rm exp}/(180 \text{ s})]$ mag. Therefore, our canonical 2 mag–extinguished SN at 25 Mpc, with an apparent $K' = 15.9$ mag, would be detected at 5 σ in about 180 s in a single background-subtracted image.

The actual observing was conducted by taking three pairs of on- and off-source frames, each pair offset by about 11″ in a different direction, all with the same exposure time. Some short exposures off-source are also taken for use in making flats. Multiple, offset frames allow us to remove cosmic rays, to correct for bad pixels, and to rule out short-lived transient sources such as asteroids and satellites.

After our galaxy images are flattened and background-subtracted, our software searches for SNe by registering each new image with a reference image and subtracting. This analysis is typically done on the same night as the new image is acquired to facilitate rapid follow-up observations. First, a median flat is made (typically from all the off-source observations during the previous nights of the run). Next, a background image is made by medianing the off-source observations. The flattened, background- and dark-subtracted frames are then fed to the subtraction software. Because the 2.″2 pixel size is large compared with the seeing, typically 0.″7–1.″0 FWHM, no seeing correction is required. The images are resampled to a finer scale (typically a factor of 5) to achieve subpixel shifting accuracy, then cross-correlated to find the optimum shift. A scaling factor is then applied by measuring a large aperture around the galaxy nucleus in each frame, so that the images have the same normalization. (Normalization by measuring isolated point sources, i.e., stars, would be more accurate. Unfortunately, detectable stars are rarely present because of our small field.) The images are then reshifted and subtracted. The

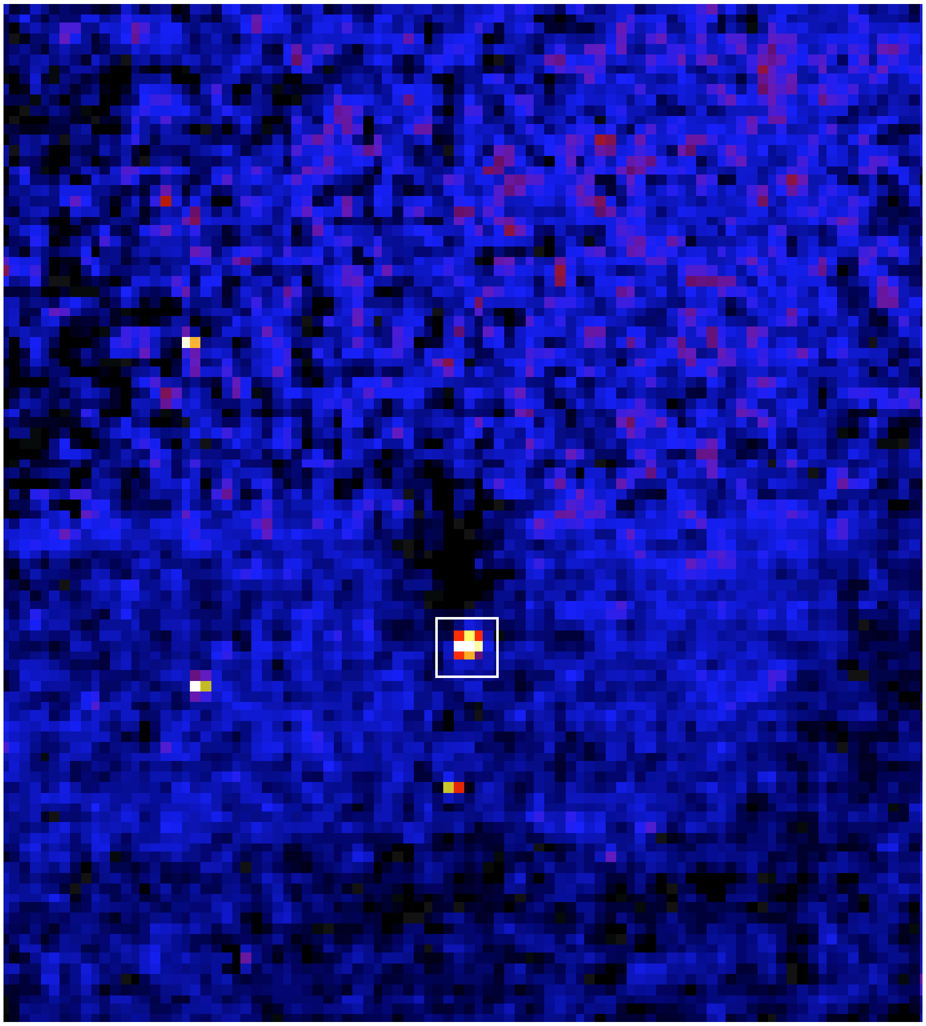

FIG. 1*c*

subtracted images are then searched for residual point sources, our SN candidates. We determine our total noise, including noise due to subtraction, directly from the subtracted images. We get good results in the disk of the galaxies, but large residuals in the bright, highly peaked nuclei of galaxies. The results are discussed quantitatively in the next section.

As proof that our system was working, we detected three unextinguished SNe after their optical discovery (1993J, 1994D, and 1994I). In Figure 1, we show the subtracted images of SN 1994I. We measured the brightness of the SN to be $K' = 12.56 \pm 0.040$ on UT 1994 April 16. The noise was estimated using the variance of background counts for apertures placed around the subtracted image at the same galaxy radius as the SN. We calibrated the measurement with observations of HD 84800, using the measurements of Elias et al. (1982) and assuming negligible corrections between the K and K' bands. The standard observations were made 7 hours before the observation of SN 1994I, a potential source of error, but the sky was clear and stable throughout the night.

6. RESULTS AND INTERPRETATION

Table A1 shows the galaxies imaged during each observing run, along with their $L_{\rm FIR}$. The number of expected SNe and observed galaxy-centuries for various subsamples of our data are given in Table 3. From our observations of 0.6×10^{10} $L_{\odot,\rm FIR}$-centuries, we can estimate that the total expected number of observed SNe in our 25 Mpc sample was 0.96–6.0 for our range of 1.6–10 FIRSRU. No extinguished SNe were discovered. All of our detected SNe were easily detected in optical observations and were therefore unextinguished. Normally, one would derive a 90% confidence upper limit of 3.8 FIRSRU (4.2 BSRU) for the extinguished-SNe rate in our 25 Mpc sample, but below we show that we were not sensitive to SNe in all locations within our galaxies. We observed a few additional galaxies with very high IR luminosity out to 50 Mpc, but here we were not sensitive to SNe with more than $A_K = 0.5$ mag. In these observations, we observed 0.98×10^{10} $L_{\odot}$ FIR-centuries, for a 90% confidence upper limit of 2.3 FIRSRU (3.4 BSRU).

With the MIRC camera, we had a choice of observing at prime focus, where we would have an image scale of 2\".2 pixel^{-1} and a field 4'.7 across, or (with some modification to the dewar) at Cassegrain focus with less than 0\".2 pixels and a field only 1% of the area at prime focus. We decided that the latter situation would be impractical, because of exposure time and because our most important galaxies, M 82 and NGC 253, barely fit the frame at prime focus. We decided it would be a mistake to throw away so much of

TABLE 3

SN RATE MEASUREMENTS

A. FIRSRU

D_{max} (Mpc)	Total Galaxy-Centuries[a]	Expected SNe at 1.7 FIRSRU	Expected SNe at 10 FIRSRU	90% Upper Limit to SN Rate[b] (FIRSRU)
15......	0.27	0.45	2.66	8.65
25......	0.60	1.02	6.00	3.83
40......	0.76	1.29	7.57	(3.04)[c]
50......	0.98	1.67	9.83	(2.34)[c]

B. BSRU

D_{max} (Mpc)	Total Galaxy-Centuries[a]	Expected SNe at 0.74 BSRU	Expected SNe at 2 BSRU	90% Upper Limit to SN Rate[b] (BSRU)
15......	0.34	0.25	0.68	6.7
25......	0.55	0.40	1.09	4.2
40......	0.66	0.49	1.32	(3.5)[c]
50......	0.68	0.50	1.36	(3.4)[c]

[a] 1 galaxy-century = 10^{10} $L_{\odot}$ measured in the indicated band, observed for a control time of 100 yr. See definition of control time in text.

[b] Here SN rate = (Poisson 90% upper limit for zero observed SNe)/(No. of galaxy-centuries observed).

[c] Here the limited sensitivity of our images permitted only $A_K = 1.3$ mag of extinction to the SNe to 40 Mpc and 0.5 mag of extinction to the SNe to 50 Mpc.

our field. However, what we gave up was the ability to search for SNe in the nuclear starburst region throughout most of our sample galaxies.

We could not search in the nuclear starburst region because our instrument had insufficient resolution. Joy, Lester, & Harvey (1987) describe the starburst region (as measured by CO emission) in M 82 as ring-shaped with a peak-to-peak diameter of 450 pc. There is no reason to expect that larger central starburst regions are common in our nearby sample, so, in the following argument, we assume the majority of our sample nuclear starburst regions are this size or smaller. Consider the implications for our images of the core-collapse SN 1994I in M 51 (8.3 Mpc away; Richmond et al. 1996; see Fig. 1) if it occurred in an extinguished nuclear starburst region. We measured 565 counts from this SN, in a 90 s image taken near maximum brightness. This optically detected SN was about 10 pixels from the galaxy center, where the subtraction noise was small (66 counts in our aperture, or 18 counts pixel^{-1}). Scaling the M 82 starburst-region size by the relative distances of M 51 and M 82 yields a radius of the starburst region of about 3 pixels in M 51. (Note that several works in this field adopt a distance of 3.2 Mpc for M 82. We use the distance to its companion M 81, 3.6 Mpc; Freedman et al. 1994.) Our subtractions are of poor quality in this central region. The standard deviation of an ensemble of apertures within a radius of 4 pixels from the galaxy center was about 140 counts. A comparison of this subtraction noise in the starburst region with the 560-count SN signal shows that we would only marginally detect (4 σ) starburst-region SNe in M 51. Since most of the galaxies in our (volume weighted) 25 Mpc sample are much more distant, SNe in these galaxies would be even fainter. The more distant the galaxy, the more sharply peaked the nucleus, and the higher the subtraction noise relative to the peak brightness. The heavily extinguished SNe (A_v = 10–20 mag) we are searching for would also have 1–2 mag of extinction even in our K' images, further reducing the signal to noise. Starburst-region SNe at distances beyond M 51 are therefore undetectable for our instrumentation, forcing our detection rate to be low regardless of the value of the nuclear SN rate. The 2″.2 pixels of the MIRC camera are too large compared with the approximately 0″.7–1″.0 FWHM seeing disk, so bright nuclei are too undersampled to yield subtractions with low noise at the nucleus, just where the SNe are predicted to be.

The productive results of this phase of our investigations are that we now have the experience and software for observing and reducing images of a large number of galaxies each night. Our observations, which find no SNe outside of starburst nuclei, also support the extinguished-SN hypothesis, that these SNe are concentrated in the nucleus. (Quantitatively, our data limit the rate of extinguished SNe outside the nucleus to less than 3.8 FIRSRU at 90% confidence, but place no useful limits on the SN rate within the nucleus.) A much smaller field covering the nucleus is therefore acceptable, making future searches much easier with currently available instruments.

7. THE NEXT STEP: A HIGHER RESOLUTION NUCLEAR SEARCH

In early 1995 we obtained the use of a NICMOS 256 × 256 array in the New Mexico IR Detector camera, which has much better noise characteristics, and discontinued observing with the MIRC. During this year, we designed and built field reimaging optics, called the Optimum Resolution Camera Adapter (ORCA), to fully sample the point-spread function (PSF). The camera dewar was enlarged to maintain these optics at cryogenic temperatures to minimize their thermal emission. This configuration yields a pixel size of 0″.29 pixel^{-1}, an appropriate match to our 0″.7–1″.0 seeing FWHM. Although our field is now only 1′.2 across, we are assured we will miss few SNe outside the nucleus, as we already have a moderately strict limit on the SN rate at galaxy radii outside the field.

Figure 2 shows an image of M 82 with the ORCA. Note that we have demonstrated good background subtraction (no anomalous structure is evident in the image, the edges are smooth and faint, etc.) even though this large, nearby galaxy fills our field and even though we need to point far from the galaxy for our background frames. In poor conditions we measure a background noise of 18.2 mag pixel^{-1} in 100 s on and off source, which permits us to measure a 15.8

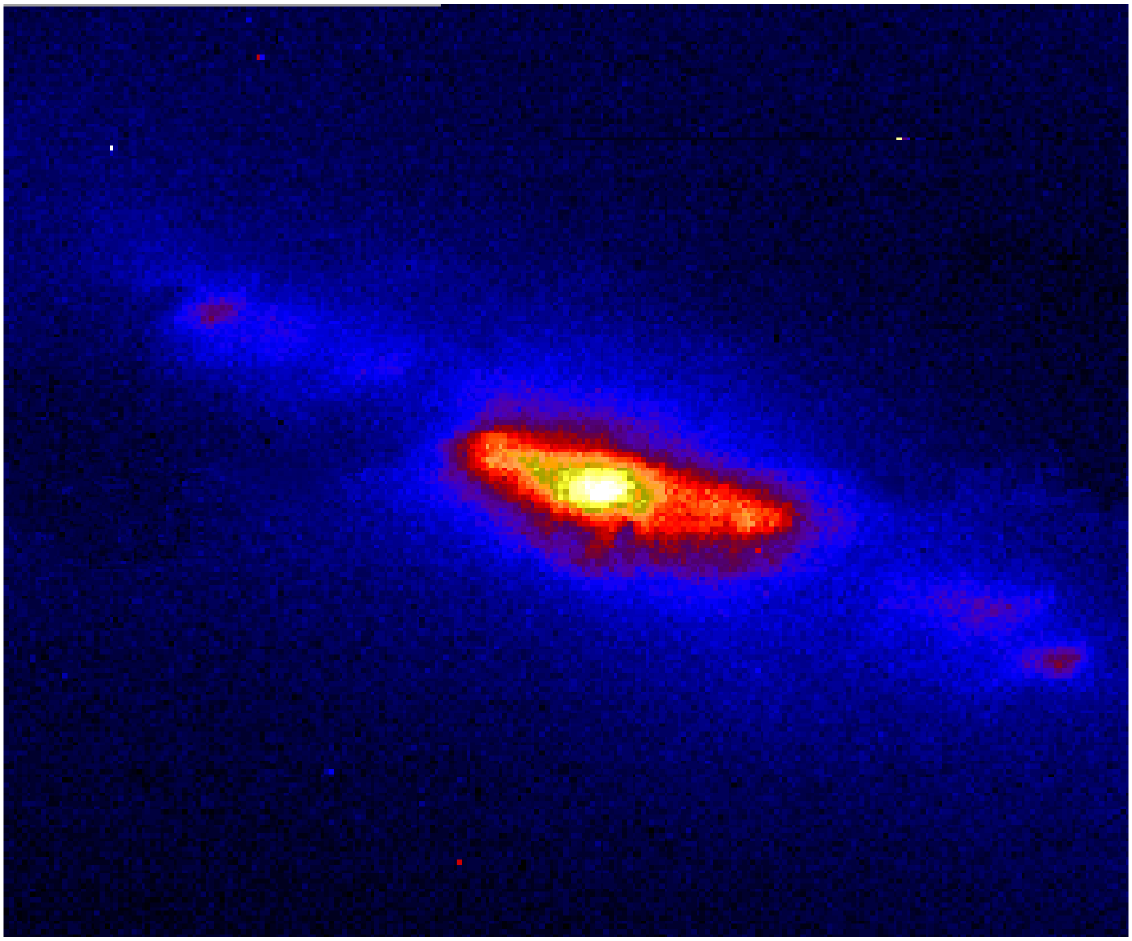

FIG. 2.—ORCA K' image of NGC 3034 (M 82) taken 1995 May 11 at the WIRO telescope. The image scale is 0".29 pixel^{-1}. North is up, east is left.[*See the electronic edition of the Journal for a color version of Fig. 2.*]

mag star at 5 σ in less than 900 s of integration. No data in typical conditions are available at this time. We also expect to increase our performance significantly by reducing the camera background through better alignment of the Lyot stop.

The higher resolution of the new camera gives us a very powerful tool for image subtraction—the ability to resolve the point-spread function (PSF). By measuring the PSF of stars near each target galaxy, we can measure the PSF for each series of galaxy images even if there are no stars in our small field. In most cases, suitable stars are available within a few arcminutes of the galaxy and may be measured in background frames. When suitable stars are too far to obtain a good background, we measure bright stars in <120 s including read time, a small increase in time compared with our 1800 s on + off source exposures. During subtraction, the new or reference image, whichever has better seeing, will be smeared to match the PSF in the other image, yielding low subtraction residuals. This subtraction and subsequent SN identification technique has been used regularly in optical supernova searches by the Berkeley group, as described in several publications (e.g., Perlmutter et al. 1997 and references therein). We have already implemented the software required to observe catalog stars for PSF measurement automatically during our galaxy observations.

A new search with the ORCA will produce a strict limit to the SN rate. Based on our 900 s integration time in poor conditions, adding read and slew times, taking 1/2 exposure time for the closer half of the sample, and a 66% acceptable weather factor, we should be able to observe 89 galaxies per typical five-night (11 hr nights) observing run. (Due to longer exposures than with the previous camera, we will only repeat observations of galaxies with SN candidates. Backgrounds are split into three exposures, adding two additional read times, so that PSF stars may be dithered for median removal from backgrounds and for good profile measurement.) Based on our projected values for camera performance (i.e., after we have aligned the Lyot stop) in more typical conditions, and conservatively assuming 1 mag worse background than achieved for other cameras at the same site, we should be able to observe 142 galaxies per run (more than would be visible in our sample). Either way, we can observe the majority of our sample visible in any month. After 3 years of operation, the discovery of no SNe would limit the extinguished-SN rate to <1.3 FIRSRU at 90% confidence, less than the most pessimistic non-optical estimate in Table 1.

8. SUMMARY

Optical measurements of the SN rate could be missing a significant fraction of SNe, particularly in the nuclei of starburst galaxies. Non-optical SN rates are, so far, derived from indirect measurements, not direct observations of SNe. Some of these non-optical rates imply much higher rates that those given by optical searches, but they vary widely. Our direct, wide-field observations in the K' band show that in our 25 Mpc *IRAS* galaxy sample, the SN rate must be less than 3.8 FIRSRU at 90% confidence outside galaxy nuclei ($>15''$ radius). This result allows future SN searches in nearby galaxies to cover only the nucleus of each galaxy (the inner $\sim$450 pc). Because the galaxy nuclei are very bright, low-residual subtractions are required for such a search. From this requirement follows the need for adequate sampling of the instrumental point-spread function. Our collaboration will proceed with such a search with the required high-resolution camera as soon as funding is available.

We note that a recent study of optical SN rates included an explicit measurement within the nuclei of starburst galaxies (Richmond et al. 1998). The authors of this work searched for changes in optical flux (Lick Observatory R_S band) consistent with SN explosions within a fixed aperture containing the nucleus of each galaxy. Because of the bright nucleus background in the apertures, the sensitivity of this technique was poor and yielded a low cumulative visibility time. With no observed SNe, the authors were only able to limit the nuclear rate of unobscured SNe to less than 12 h^2 BSRU for Type Ibc and less than 7 h^2 BSRU for Type II. As with other optical measurements, however, the study was insensitive to heavily obscured SNe. The unobscured SN rate in the very important nuclear region of starbursts therefore remains an open question of great interest.

The authors would like to thank N. Panagia for making significant contributions of data and analysis to this paper. We also thank H. Thronson for valuable scientific input, and generous donation of telescope time to our project. Special thanks are given to the faculty, students, and staff of the University of Wyoming Department of Physics and Astronomy in supporting B. G. during his visits and to the staff of WIRO for their excellent technical support of this project. We acknowledge receipt of funding from the NASA GRO Guest Observer Program, the Lawrence Berkeley National Laboratory (LBNL) Physics Division, and the LBNL Institute for Nuclear and Particle Astrophysics.

APPENDIX

Table A1 lists our observations.

TABLE A1

TABLE OF OBSERVATIONS

Galaxy	D (Mpc)	$\log L_{FIR}$	1993 Feb	1993 Mar	1993 Jul	1993 Oct	1993 Dec	1994 Feb	1994 Mar	1994 Apr	1994 May	1994 Jun
NGC 150	21.2	9.96				X	X					
NGC 157	22.0	10.35			X		X					
NGC 247	3.6	8.67			X	m	X					X
NGC 253	3.6	10.6				X	X					
NGC 278	11.8	9.62			X	X	X					X
NGC 337	22	10			X							
NGC 578	22.6	9.81			X							
NGC 598	0.8	9.11			X	m	X	X			X	X
NGC 613	19.8	10.31				X	X					
NGC 628	8.7	9.87			m	X	X	X				X
NGC 660	11.5	10.38			X	X	X	X				
NGC 693	21.2	9.86			X							
NGC 701	18.9	9.8			X							
NGC 772	33.1	10.47			X							
NGC 891	9.6	9.83			X	X	X		X			
NGC 908	17.8	10.23				X	X					
NGC 925	9.4	8.99			X	m	m	X				
NGC 972	20.6	10.5			X	X	X	X				X
NGC 1022	18.5	10.18			X	m	X					
Maffei II	5.0	9.72			m	m		X	X			X
NGC 1055	12.6	10.08			X	m		X				
NGC 1056	9.3	9.03			X	m	X		X			
NGC 1068	14.4	10.9			X		X	X				
NGC 1084	17.1	10.34			X	m		X				
NGC 1087	19.0	10.1				X						
NGC 1156	5.0	8.54			X		X		X			
NGC 1187	16.3	9.9										
NGC 1232	20.0	10.3				m	X					
IC 1953	22.1	10										
NGC 1385	17.5	10.1				m	X					
NGC 1415	17.7	9.7				X						
NGC 1421	25.5	10.2				X						
IC 342	4.7	10.06	X		X	X	X	X	X			
UGC 2855	15.4	10.34	X		X	X	X	X	X			
UGC 2866	16.4	10.38			X	X		X	X	X		

TABLE A1—*Continued*

Galaxy	D (Mpc)	log L_{FIR}	1993 Feb	1993 Mar	1993 Jul	1993 Oct	1993 Dec	1994 Feb	1994 Mar	1994 Apr	1994 May	1994 Jun
NGC 1482	19.6	10.4				X	X					
UGC 2953	12.0	9.34			X	X	m					
NGC 1530	32	10.35			X							
NGC 1569	1.6	8.6			X	X	X					
NGC 1637	8.9	9.13				m	X					
UGC 3190	20.8	9.74										
NGC 1832	25.8	10.05										
NGC 1964	22.3	9.99										
0553+03	10.3	9.19										
NGC 2139	24.5	9.99				m						
NGC 2146	17.2	10.69	m	m		X	X	X		X		
0616−08	10.1	9.57				X	X					
NGC 2283	11.3	9.38				m	X					
NGC 2276	32.3	10.49				X						
NGC 2403	4.2	9.31		m		m	X	X		X		
0834−26	10.5	9.89				m				X		
NGC 2681	13.3	9.48									X	
NGC 2748	20.0	10.2				m	X					
NGC 2798	23.4	10.59	X	m		X	X	X				
NGC 2820	22.5	10.02										
NGC 2841	14.3	9.46										
NGC 2903	6.3	9.93	X	X		X	X	X	X	X		
NGC 2964	21.9	10.2		X								
NGC 2976	3.4	8.62						X			X	
NGC 2992	30.5	10.46									X	
NGC 2985	17	10.1										
NGC 3044	20.6	10.06		X								
NGC 3031	3.6	9.39	X	X		X	X	X	X	X		
NGC 3034	3.6*	10.45	X	X		X		X	X	X		
NGC 3067	24.2	10.2										
NGC 3079	20.4	10.63	X	X		X	X		X		X	
NGC 3077	3.4	8.6			X			X	X	X		X
NGC 3166	22	9.93										
NGC 3169	19.7	9.98										
NGC 3147	37.6	10.74										
NGC 3177	21.1	10.1		X								
NGC 3184	8.7	9.43						X	X		X	
NGC 3198	10.8	9.52										
NGC 3227	20.6	9.95										
NGC 3294	26.7	10.21		X								
NGC 3310	18.7	10.39				X	X		X	X		
NGC 3344	6.1	8.98						X				
NGC 3351	8.1	9.42				X		X	X	X		
NGC 3353	16.8	9.57										
NGC 3368	8.1	9.45				X						
NGC 3395/6	27.4	10.31										
NGC 3424	19.9	10.22		X			X				X	
NGC 3432	10.9	9.32										
NGC 3437	17.2	10.23						X			X	
NGC 3448	18.4	9.96										
NGC 3486	7.4	9.06						X				
NGC 3504	20.7	10.55	X			X		X		X		
NGC 3511	16.3	9.94										
NGC 3521	7.2	9.94		m		X	X	X	X			X
NGC 3556	14.1	10.3				X	X		X	X		X
NGC 3583	28.5	10.42										
NGC 3593	5.5	9.16			X	X	X	X				
NGC 3623	13.5	9.22				X						
NGC 3627	6.6	10.25	X	X	X	X	X	X	X	X		X
NGC 3628	7.7	10.18	X	X	X	X	X	X	X	X		
NGC 3631	15.5	10.21			X			X				X
NGC 3655	19.7	9.85										
NGC 3672	24.7	10.37							X	X	X	
NGC 3675	12.8	9.86										
NGC 3683	22.1	10.49				X	X		X			X
NGC 3690	42.1	11.72	X	X	X	X	X					

TABLE A1—*Continued*

Galaxy	*D* (Mpc)	log L_{FIR}	1993 Feb	1993 Mar	1993 Jul	1993 Oct	1993 Dec	1994 Feb	1994 Mar	1994 Apr	1994 May	1994 Jun
NGC 3726	16.7	9.87										
NGC 3735	35.9	10.58			X							
NGC 3810	17.7	10.07			X							
NGC 3877	17.4	9.85			X							
NGC 3885	26	10.3										
NGC 3887	15.1	9.8										
NGC 3893	17	10.22								X		
NGC 3938	17	9.71										
NGC 3949	17	9.89										
NGC 3953	20.2	10.24										X
NGC 3955	17.9	10.01										
NGC 3981	22.9	10.22										
NGC 3982	14.8	9.98										
NGC 4013	11.1	9.84			X					X		
NGC 4027	22.4	10.4						X		X		
NGC 4030	19.5	10.26			X			X		X	X	X
NGC 4038/9	20.8	10.81						X	X			
NGC 4041	16.5	10.34							X	X		
NGC 4045	26.6	10.28										
NGC 4051	9.5	9.53			X			X		X		
NGC 4085	10.0	9.61			X			X		X		
NGC 4088	10.2	10.19		X	X	X	X	X		X	X	
NGC 4096	8.8	9.49			X			X		X	X	
NGC 4100	14.3	10.08										
NGC 4102	11.5	10.52			X	X	X	X	X			X
NGC 4123	18.0	9.68										
NGC 4157	10.3	10.11			X	X	X	X	X	X		
NGC 4192	12.4	9.68			X							
NGC 4216	21.9	9.55			X							
NGC 4258	6.8	9.76						X		X	X	
NGC 4298	14.9	9.85			X							
NGC 4303	20.9	10.85			X		X	X		X		
NGC 4321	21.0	10.33			X		X	X		X		X
NGC 4332	37.9	10.57			X							
NGC 4369	14	9.88			X							
NGC 4383	22.6	9.77			X							
NGC 4388	18.8	9.94			X							
NGC 4402	3.2	9.81			X		X	X		X		X
NGC 4414	9.7	10.14			X		X	X		X		
NGC 4418	27.3	11			X			X				
NGC 4419	16.8	9.84			X							
NGC 4438	16.8	9.77										
NGC 4490	7.8	9.8			o			X	X			
NGC 4526	16.8	9.8								X		
NGC 4527	23.2	10.87			X		X	X		X		
NGC 4532	20.5	9.97										
NGC 4535	16.1	9.9										
NGC 4536	24.3	10.83			X		X	X				
NGC 4559	13	9.79										
NGC 4565	13	10.01			X							
NGC 4569	11.5	9.67			X							
NGC 4594	15	10.12			X							
NGC 4631	8.2	10.09	X	X	X		X	X	X	X		
NGC 4651	21.2	9.93			X							
NGC 4654	16.2	10.07										
NGC 4666	21.9	10.93			X		X	X		X		X
NGC 4691	23.8	10.28								X		
NGC 4710	15.0	9.73										
NGC 4725	23.3	9.82										
NGC 4736	4.3	9.52			X		X	X	X			X
NGC 4781	16.9	10.1										
NGC 4808	16.1	9.7										
NGC 4818	14.0	9.67										
NGC 4826	5.5	9.24			X		X	X		X		X
NGC 4845	17.4	9.94			X							
NGC 4900	17.7	9.69										

TABLE A1—*Continued*

Galaxy	D (Mpc)	log L_{FIR}	1993 Feb	1993 Mar	1993 Jul	1993 Oct	1993 Dec	1994 Feb	1994 Mar	1994 Apr	1994 May	1994 Jun
NGC 5005......	12.7	10.5	X		X	X	X	X	X	X		X
NGC 5033......	11.7	10.4	X		X	X	X	X	X	X		X
NGC 5055......	6.6	10.01	X	X	X			X				X
NGC 5170......	25.7	9.3										
NGC 5194......	8.3*	10.49	X	X	X			X	X	X		X
NGC 5195......	9.3	9.47			X		X	X				X
NGC 5236......	9.9	10.77						X	X			
NGC 5248......	15.4	10.22			X		X	X		X		X
NGC 5457......	8.1	10.32	X		X		X	X	X			X
NGC 5506......	24.1	10.2										
NGC 5678......	25.7	10.52			X		X	X		X		X
NGC 5676......	28.1	10.67			X			X	X			X
NGC 5690......	23.3	10.24			X							
NGC 5713......	25.3	10.69			X			X				
NGC 5719......	19.7	10.18			X							
NGC 5775......	22.3	10.69			X		X	X				X
NGC 5792......	25.7	10.4			X							
NGC 5866......	9.0	9.66			X	X		X			X	X
NGC 5861......	25	10.38			X							X
NGC 5900......	34	10.54			X	X						X
NGC 5907......	8.9	10.16	X	X	X	X	X	X		X		X
NGC 5915......	31	10.48			X							X
NGC 5929......	35	10.55		m	X	X						
NGC 5937......	33	10.61			X					X		X
NGC 5953......	26	10.46		X	X	m						X
UGC 9913......	72.7	12.12			X	m						
NGC 5962......	26	10.45			X	m						X
NGC 6015......	16.5	9.6			X							X
NGC 6181......	32	10.57			X	X						X
NGC 6217......	23.9	10.22			m	X						X
NGC 6503......	6.1	8.97			X	X	X					X
NGC 6574......	30	10.47			X	X						X
NGC 6643......	25.5	9.96			X							
NGC 6764......	31.7	10.18			X	m						
NGC 6814......	21	9.74				m						X
NGC 6835......	22.8	10.06			X	X	X					X
NGC 6946......	5.5	9.97		X	X	X	X					X
NGC 6951......	24.1	10.06			X		X					X
NGC 7331......	14.3	10.19			X	X	X					X
NGC 7448......	29	10.33			X	X	X					X
NGC 7465......	26	10.03			X	X	X					X
NGC 7469......	66	11.4			m	X	X					
NGC 7479......	32	10.55			X	X	X					X
NGC 7541......	36	10.83			X	X	X					X
NGC 7625......	22	10.12			X	X	X					X
NGC 7640......	13.0	9.17			X	X	X					X
NGC 7673......	45	10.39			m	m	X					
NGC 7678......	47	10.64			X	m	X					
NGC 7771......	58	11.2			X		X					
NGC 7714......	37	10.51			X		m					

NOTES.—An "X" indicates a successful observation. An "m" indicates a marginal observation, usually due to poor transparency. Distances are taken from Soifer et al. 1987, and where not in Soifer et al., from Tully 1988. An asterisk indicates a distance from another source, as explained in the text. L_{FIR} are taken from Soifer et al. 1987, or where not present, they were generated from the given distance and the Cataloged Galaxies in the *IRAS* Survey, Version 2 (1989).Our values of L_B were taken directly from Tully 1988 except in a few cases and so are not reproduced here. The exceptions are: Maffei II and IC 342, M_B taken from Krismer, Tully, & Gioia 1995; NGC 1482, extinction-corrected B from Lauberts & Valentijn 1989; 0616−08, where a B-value could not be found; NGC 4402, 5900, 5929, 5937, and 7678, B taken from the RC3 (de Vaucouleurs et al. 1991); and NGC 3690, B taken from Richmond et al. 1998.

REFERENCES

Allen, M. L., & Kronberg, P. P. 1998, ApJ, 502, 218

Antonucci, R. R. J., & Ulvestad, J. S. 1988, ApJ, 330, L97

Bahcall, J. N. 1989, Neutrino Astrophysics (Cambridge: Cambridge Univ. Press)

Buta, R. J. 1982, PASP, 94, 578

Capellaro, E., & Turatto, M. 1988, A&A, 190, 10

Cardelli, J. A., Clayton, G. C., & Mathis, J. S. 1989, ApJ, 345, 245

Cataloged Galaxies and Quasars Observed in the *IRAS* Survey, Version 2. 1989, prepared by C. J. Lonsdale, G. Helou, J. Good, & W. Rice (Pasadena: JPL)

Cowan, J. J., Roberts, D. A., & Branch, D. 1994, ApJ, 434, 128

de Vaucouleurs, G., de Vaucouleurs, A., Corwin, H. G., Jr., Buta, R. J. Paturel, G., & Fouqué, P. 1991, Third Reference Catalogue of Bright Galaxies (New York: Springer) (RC3)

Dwek, E., et al. 1983, ApJ, 274, 168
Elias, J. H., Frogel, J. A., Matthews, K., & Neugebauer, G. 1982, AJ, 87, 1029
Elias, J. H., Matthews, K., Neugebauer, G., & Persson, S. E. 1985, ApJ, 296, 379
Engelbracht, C. W., Rieke, M. J., Rieke, G. H., Kelly, D. M., & Achtermann, J. M. 1998, ApJ, 505, 639
Evans, R., van den Bergh, S., & McClure, R. D. 1989, ApJ, 345, 752
Freedman, W. L., et al. 1994, ApJ, 427, 628
Joy, M., Lester, D. F., & Harvey, P. M. 1987, ApJ, 319, 314
Krismer, M., Tully, R. B., & Gioia, I. M. 1995, AJ, 110, 1584
Kronberg, P. P., Biermann, P., & Schwab, F. R. 1985, ApJ, 291, 693
Kronberg, P. P., & Sramek, R. A. 1985, Science, 227, 28
Kronberg, P. P., & Wilkinson, P. N. 1975, ApJ, 200, 430
Lauberts, P., & Valentijn, E. A. 1989, The Surface Photometry Catalogue of the ESO-Uppsala Galaxies (Garching: ESO)
Miller, D. L., & Branch, D. 1990, AJ, 100, 530 (MB90)
Muller, R. A., Newberg, H. J. M., Pennypacker, C. R., Perlmutter, S., Sasseen, T. P., & Smith, C. K. 1992, ApJ, 384, L9
Muxlow, T. W. B., Pedlar, A., Wilkinson, P. N., Axon, D. J., Sanders, E. M., & de Bruyn, A. G. 1994, MNRAS, 266, 455
Perlmutter, S., et al. 1997, in Thermonuclear Supernovae, ed. P. Ruiz-Lapuente, R. Canal, & J. Isern (NATO ASI Ser. C, 486) (Dordrecht: Kluwer), 749
Richmond, M. W., Filippenko, A. V., & Galisky, J. 1998, PASP, 110, 553
Richmond, M. W., et al. 1996, AJ, 111, 327
Rieke, G. H., Lebofsky, M. J., Thompson, R. I., Low, F. J., & Tokunaga, A. T. 1980, ApJ, 238, 24
Schaller, G., Schaerer, D., Meynet, G., & Maeder, A. 1992, A&AS, 96, 269
Soifer, B. T., Sanders, D. B., Madore, B. F., Neugebauer, G., Danielson, G. E., Elias, J. H., Lonsdale, C. J., & Rice, W. L. 1987, ApJ, 320, 238
Suntzeff, N. B., & Bouchet, P. 1991, in Supernovae, ed. S. E. Woosley (New York: New York), 3
Tully, R. B. 1988, Nearby Galaxies Catalog (Cambridge: Cambridge Univ. Press)
Ulvestad, J. S., & Antonucci, R. J. R. 1994, ApJ, 424, L29
Van Buren, D., & Greenhouse, M. A. 1994, ApJ, 431, 640
Van Buren, D., Jarrett, T., Terebey, S., Beichman, C., Shure, M., & Kaminski, C. 1994, IAU Circ. 5690
Van Buren, D., & Norman, C. A. 1989, ApJ, 336, L67
van den Bergh, S., & Tammann, G. A. 1991, ARA&A, 29, 363
Woosley, S. E., & Weaver, T. A. 1986, ARA&A, 24, 205